FINAL REPORT

SCOUR AT COMPLEX PIERS

FLORIDA DEPARTMENT OF TRANSPORTATION
RESEARCH OFFICE
605 SUWANNEE STREET
TALLAHASSEE, FL 32399-0450

SUBMITTED BY:

D. MAX SHEPPARD
CIVIL AND COASTAL ENGINEERING DEPARTMENT
UNIVERSITY OF FLORIDA
GAINESVILLE, FLORIDA 32611

FDOT AND UF PROJECT NUMBERS

FDOT: BC354 RPWO 35
UF:4910 45-04-799

MARCH 2003

TABLE OF CONTENTS

LIST OF SYMBOLS

b	=	single pile diameter/width,
b_{col}	=	width of column,
b_{pc}	=	width of pile cap,
D_{16}	=	sediment size for which 16 percent of bed material is finer,
D_{50}	=	median sediment grain diameter,
D_{84}	=	sediment size for which 84 percent of bed material is finer,
D^*	=	effective diameter,
f	=	protrusion of pile cap upstream of pile column,
H_{col}	=	height of bottom of pier column above bed,
H_{pc}	=	height of bottom of pile cap above bed,
H_{pg}	=	height of top of piles above bed,
K_h	=	coefficient that accounts for the hight of the piles above the bed in a pile group,
K_s	=	pier shape factor,
K_{sp}	=	coefficient that accounts for pile spacing in a pile group,
K_α	=	skew angle coefficient,
K_m	=	coefficient that accounts for the number of piles inline with the flow for small skew angles,
m	=	number of piles inline with the unskewed flow in a pile group,
n	=	number of piles normal to the unskewed flow in a pile group,
s	=	distance between centerlines of adjacent piles in pile group,
T	=	thickness of pile cap,
V	=	depth averaged velocity;
V_c	=	depth averaged velocity at threshold condition for sediment motion (sediment critical velocity),
w_{pi}	=	projected width of an unobstructed single pile in a pile group,
W_p	=	projected width of pile group,
y_s	=	scour depth,

y_0 = unscoured approach water depth,

y_1 = water depth after aggradation and contraction scour,

y_{1max} = maximum water depth after aggradation and contraction scour that impacts scour,

y_2 = water depth after aggradation, contraction scour and column scour,

y_{2max} = maximum water depth after aggradation, contraction scour and column scour that impacts scour,

y_3 = water depth after aggradation, contraction scour, column scour and pile cap scour,

y_{3max} = maximum water depth after aggradation, contraction scour, column scour and pile cap scour that impacts scour,

α = flow skew angle (approach angle to axis of pier),

μ = dynamic viscosity of water,

ρ_s = mass density of sediment,

ρ_w = mass density of water,

σ = standard deviation of sediment particle size distribution, $\sqrt{\frac{D_{84}}{D_{16}}}$,

τ = bed shear stress,

τ_c = critical bed shear stress.

SCOUR AT COMPLEX PIERS

Introduction

This report contains the results of experiments performed and analyses conducted for the purpose of predicting sediment scour at complex bridge piers. The data used in the analyses were from experiments conducted 1) by the principal investigator at the University of Florida and 2) by J. Sterling Jones at the FHWA Turner Banks Laboratory in McLean Maryland. The methodology used in the analyses is discussed first, followed by the empirical relationships need in the analyses. These relationships were obtained from the experimental data presented in Appendix A. The methods and procedures described in this report apply to structures similar to those illustrated in Figure 1. Many new and existing pier designs are covered by this generic design. It is recommended that physical model tests be conducted for other pier designs if design scour depths are an issue.

Methodology for Estimating Local Scour Depths at Complex Piers

This section presents a methodology for estimating equilibrium local scour depths at complex pier geometries under steady flow conditions. This methodology applies to structures that are composed of up to three components as shown in Figure 1. In this report these components are referred to as the 1) Column, 2) Pile Cap and 3) Pile Group.

The methodology for predicting local scour depths at complex pier geometries begins with the following three assumptions:

1- The structure can be divided into no more than three components as shown in Figures 1 and 2.
2- The equilibrium local scour depth for the total structure can be estimated by summing the scour produced by each of the structure components.
3- For scour calculation purposes, each component can be replaced by a single, surface penetrating, circular pile with an effective diameter, D^*, that depends on the shape, size and location of the component and its orientation relative to the flow.

The functional dependence of the effective diameter for each component on its shape, size and location has been established empirically through numerous experiments performed by J. Sterling Jones at the FHWA Turner Fairbanks Laboratory in McLean, Virginia, and by D. Max Sheppard in the Hydraulics Laboratory at the University of Florida and in the Hydraulics Laboratory at the Conte USGS-BRD Research Center in Turners Falls, Massachusetts.

The methodology described here is only for estimating Local Scour Depths. General scour, aggradation and/or degradation, and contraction scour depths must be established prior to using this procedure. The information needed to compute local scour depths at complex piers is summarized below:

1. General scour, aggradation and/or degradation and contraction scour depths.
2. External dimensions of all pier components including their positions relative to the unscoured channel bed.
3. Sediment properties (mass density, median grain diameter and grain diameter distribution).
4. An estimate of the relative bed roughness (roughness height divided by the median grain diameter).
5. Water properties (mass density, ρ, and dynamic viscosity, μ)
6. Water depth and depth-averaged flow velocity just upstream of the structure.

Local Scour Depth Calculation Procedure

The procedure involves decomposing the structure into it's (up to three) components, computing the scour depth produced by each component (starting with the uppermost component and working down) and summing these depths. Adjustments to both the bed elevation and the depth-averaged velocity are made after each component scour is computed. As stated above, the local scour depth at the composite pier is the sum of the scour depths for the individual components. The step-by-step procedure for computing the equilibrium scour depth for each component is presented below.

1. Divide the pier into its components

   Divide the complex pier into its components as shown in Figure 2. Note that y_0 is the initial water depth before aggradation/degradation and contraction scour.

2. Sum the aggradation/degradation and contraction scour depths

   Sum the computed scour depths produced by aggradation/degradation and contraction scour and adjust the bed elevation accordingly. That is, if there is a net lowering of the bed due to these mechanisms then the bed elevation must be lowered by this amount and increase the initial, unscoured water depth, y_0, to y_1.

$$y_1 = y_0 + (\text{degradation} + \text{contraction scour}) \quad (1)$$

3. Compute the Critical Depth Averaged Velocity, V_c, (i.e. the velocity that will initiate sediment motion on a flat bed for the given upstream water depth and sediment properties). The critical velocity for a given situation can be determined from the equations or plots given in Appendix B of this report. These equations/plots are based on Shield's curve. Note that this value of critical velocity is used for all of the following calculations.

4. Compute the live bed peak scour velocity, V_{lp}, from the equations or plots for this purpose presented in Appendix B.

5. Compute the local scour depth due to the **Column**

   a. Compute the value of the parameter, $y_{1(max)}$, (this places a limit on the magnitude

of the water depth for the column scour calculations).

$$y_{1(max)} = \begin{cases} y_1 & \text{for } y_1 \le 2.5b_{col} \\ 2.5b_{col} & \text{for } y_1 > 2.5b_{col} \end{cases} \quad (2)$$

where
$y_1 \equiv y_0 + (\text{degradation} + \text{contraction scour})$, and
$b_{col} \equiv$ width of column (Figure 2)

b. Determine the flow skew angle coefficient, K_α, which depends on the flow direction and pier orientation. K_α can be computed using the following equation:

$$K_\alpha = \frac{b_{col}\cos(\alpha) + L_{col}\sin(\alpha)}{b_{col}} \quad (3)$$

where
$\alpha \equiv$ flow skew angle, (see Figure 3), and
$L_{col} \equiv$ horizontal length of column (see Figure 2).

c. Obtain the effective diameter of the column, D^*_{col}, from Figure 4 or the following equation:

$$D^*_{col} = K_\alpha b_{col} \exp\left\{ \begin{array}{l} -0.71 - 0.59\left(\frac{f}{b_{col}}\right)^2 + 0.265\left(\frac{f}{b_{col}}\right)^{2.5} - 0.29\left(\frac{f}{b_{col}}\right)^{0.5} \\ \\ -1.73\left(\frac{H_{col}}{y_{1(max)}}\right) - 2.8\left(\frac{H_{col}}{y_{1(max)}}\right)^2 \end{array} \right\} \quad (4)$$

where
$D^*_{col} \equiv$ effective diameter/width of the column (i.e. the diameter/width of a water surface penetrating circular pile that will experience the same local scour depth as the column,

f ≡ distance between the leading edge of the column and the leading edge of the pile cap (see Figure 2), and

H_{col} ≡ distance from the adjusted bed to the bottom of the column.

NOTE: If $\frac{H_{col}}{y_{1(max)}}$ is greater than 1, set it equal to 1.

d. Compute the Shape Factor for the column (which depends on the shape of the column and the flow skew angle) using the following equation:

$$K_s \equiv \begin{cases} 1.0 & \text{for circular or rounded nose columns} \\ 0.9 + 0.66 \left| \alpha - \frac{\pi}{4} \right|^4 & \text{for square nose columns} \end{cases} , \quad (5)$$

where

K_s ≡ shape coefficient to account for the shape of the leading edge of the column, and

α ≡ flow skew angle in radians.

e. Knowing D^*_{col}, D_{50}, y_1, V_1, V_c, V_{lp}, and K_s, the scour depth created by the column, $y_{s(col)}$, can be estimated using single pile equilibrium scour depth prediction equations such as those given in Appendix B.

6. Compute the local scour depth due to the **Pile Cap**

a. Lower the bed elevation (and increase the water depth) by one-half the scour depth produced by the Column, $y_{s(col)}$,

$$y_2 = y_1 + \frac{y_{s(col)}}{2} . \quad (6)$$

b. Adjust the velocity to account for the increased cross-sectional area using the following equation:

$$V_2 = V_1 \frac{y_1}{y_2} . \quad (7)$$

c. Compute the value of the parameter, $y_{2(max)}$, (this places a limit on the magnitude of the water depth for the pile cap scour calculations) using the following equation:

$$y_{2(max)} = \begin{cases} y_2 & \text{for } y_2 \le 2.5 b_{pc} \\ 2.5 b_{pc} & \text{for } y_2 > 2.5 b_{pc} \end{cases}, \tag{8}$$

where
b_{pc} ≡ width of the pile cap.

d. Compute the Flow Skew Angle Coefficient, K_α, for the pile cap using the following equation:

$$K_\alpha = \frac{b_{pc} \cos(\alpha) + L_{pc} \sin(\alpha)}{b_{pc}}, \tag{9}$$

where
L_{pc} ≡ Horizontal length of the pile cap, and
α ≡ flow skew angle.

e. Knowing the pile cap thickness, T, the height of the bottom of the pile cap above the "adjusted" bed, H_{pc}, the width of the pile cap, b_{pc}, and $y_{2(max)}$, the effective diameter of the pile cap, D^*_{pc}, can be obtained from Figure 5 or the following equation:

$$D^*_{pc} = K_\alpha b_{pc} exp\left[-2.7 + 0.5 \ln_e \left(\frac{T}{y_{2(max)}} \right) - 2.8 \left(\frac{H_{pc}}{y_{2(max)}} \right)^3 + 1.76 \exp\left(-\frac{H_{pc}}{y_{2(max)}} \right) \right], \tag{10}$$

where
D^*_{pc} ≡ effective diameter/width of the pile cap (i.e. the diameter/width of a water surface penetrating pile (with the same shape as the pile cap) that will experience the same local scour depth as the pile cap,
T ≡ thickness of the pile cap for completely submerged pile cap or the depth of submergence of a partially submerged pile cap , and
H_{pc} ≡ distance between the adjusted bed and the bottom of the pile cap.

NOTE: Neither $\frac{T}{y_{2\,(max)}}$ nor $\frac{H_{pc}}{y_{2\,(max)}}$ can exceed the value of 1.0. If the computed value is greater than 1.0, set it equal to 1.0.

f. Compute the Shape Factor for the pile cap (which depends on the shape of the pile cap and the flow skew angle) using the following equation:

$$K_s \equiv \begin{cases} 1.0 & \text{for circular or rounded nose pile caps} \\ 0.9 + 0.66 \left| \alpha - \frac{\pi}{4} \right|^4 & \text{for square nose pile caps} \end{cases} . \qquad (11)$$

g. Knowing D^*_{pc}, D_{50}, y_2, V_1, V_c, V_{lp}, and K_s, the scour depth created by the pile cap, $y_{s\,(pc)}$, can be estimated using single pile, equilibrium scour depth prediction equations such as those given in Appendix B. Note that the structure shape factor is used in the scour depth calculation.

7. Compute the local scour depth due to the **Pile Group**

a. Lower the bed elevation (and increase the water depth) by one-half the scour depth produced by the Pile Cap, $y_{s\,(pc)}$,

$$y_3 = y_2 + \frac{y_{s(pc)}}{2} . \qquad (12)$$

b. Adjust the velocity to account for the increased cross-sectional area using the following equation:

$$V_3 = V_2 \frac{y_2}{y_3} . \qquad (13)$$

c. Determine the value of the coefficient, K_m, that accounts for the number of piles in the direction of the unskewed flow. Note that this coefficient also depends on the pile centerline spacing, s, normalized by the single pile diameter/width, b (i.e.

K_m depends on $\frac{s}{b}$ as well as the number of piles in the unskewed flow direction, m).

$$K_m \equiv \begin{cases} f_1(m)\, f_2\left(\frac{s}{b}\right) & \text{for flow skew angle, } \alpha \le 3 \text{ degrees} \\ 1 & \text{for } \alpha > 3 \text{ degrees} \end{cases}, \tag{14}$$

$$f_1 \equiv \begin{cases} 0.875 + 0.125m & 1 \le m \le 5 \\ 1.5 & 5 < m \end{cases}, \tag{15}$$

$$f_2 \equiv \begin{cases} a_0 + a_1\left(\frac{s}{b}\right) & 1 \le \left(\frac{s}{b}\right) \le 3 \\ a_2 + a_3\left(\frac{s}{b}\right) & 3 \le \left(\frac{s}{b}\right) \le 10 \\ a_2 + a_3(10) & 10 < \left(\frac{s}{b}\right) \end{cases}, \tag{16}$$

where

$a_0 \equiv -0.5 + 1.5\left(\frac{1}{f_1}\right)$,

$a_1 \equiv 0.5 - 0.5\left(\frac{1}{f_1}\right)$,

$a_2 \equiv 1.429 - 0.429\left(\frac{1}{f_1}\right)$ and

$a_3 \equiv -0.143 + 0.143\left(\frac{1}{f_1}\right)$.

d. Determine the "projected width" of the piles, W_p. This is the sum of the non-overlapping projections of the piles in the **first two rows and the first column** onto a vertical plane normal to the flow (Figure 3). The first column is the upstream column for piers skewed to the flow.

e. Determine the coefficient that accounts for the pile spacing, K_{sp}. Knowing the

centerline spacing between the piles, s, and the pile width, b, K_{sp} can be obtained from Figure 6 or the following equation:

$$K_{sp} = 1 - \frac{4}{3}\left(1 - \frac{w_{pi}}{W_p}\right)\left(1 - \frac{1}{\left(\frac{s}{b}\right)^{0.6}}\right), \tag{17}$$

where
w_{pi} ≡ projected width of an unobstructed single pile in the group and
W_p ≡ the projected width defined in 7.d. above.

See Figure 6 for a plot of this function.

f. If the top of the piles are at or above the water surface set $K_h = 1.0$ and advance to 7.i. Otherwise estimate the effective diameter/width of the pile group using the following equation:

$$D^*_{pg} \approx \sqrt{\frac{W_p K_m H_{pg}}{5}}, \tag{18}$$

where
H_{pg} ≡ Distance from the adjusted bed to the top of the piles .

g. Compute the value of the parameter, $y_{3(max)}$, using the following equation (this places a limit on the magnitude of the water depth for the pile group scour calculations):

$$y_{3(max)} = \begin{cases} y_3 & \text{for } y_3 \le 2.5D^*_{pg} \\ 2.5D^*_{pg} & \text{for } y_3 > 2.5D^*_{pg} \end{cases}. \tag{19}$$

h. If the tops of the piles in the group are at or above the water surface set $K_h = 1$ and proceed to the next step (7.i.). If the tops of the piles are submerged (i.e. if H_{pg} is less than $y_{3(max)}$) this will influence the scour depth produced by the group.

The coefficient that accounts for the height of the pile group above the adjusted bed, K_h, can be obtained from Figure 7 or evaluated using the following equation:

$$K_h \equiv 3.08\left(\frac{H_{pg}}{y_{3\,(max)}}\right) - 5.23\left(\frac{H_{pg}}{y_{3\,max)}}\right)^2 + 5.25\left(\frac{H_{pg}}{y_{3\,(max)}}\right)^3 - 2.10\left(\frac{H_{pg}}{y_{3\,(max)}}\right)^4. \qquad (20)$$

NOTE: If $\left(\frac{H_{pg}}{y_{3\,(max)}}\right)$ is greater than 1, set it equal to 1.

See Figure 7 for a plot of this function.

i. Knowing W_p, K_{sp}, K_m, and K_h, the effective diameter of the pile group can be determined from the following equation:

$$D^*_{pg} = K_m K_{sp} K_h W_p \qquad (21)$$

where

$D^*_{pg} \equiv$ effective diameter/width of the pile group (i.e. the diameter/width of a water surface penetrating single circular pile that will experience the same local scour depth as the pile group).

j. If the tops of the piles in the group are at or above the water surface proceed to the next step (7.k.). If the tops of the piles are submerged compute the percent difference between the value of D^*_{pg} computed in section 7.i and the estimated D^*_{pg} value from section 7.f using:

$$\text{Percent Difference} = \left|\frac{D^*_{pg}(\text{from 7i}) - D^*_{pg}(\text{from 7f})}{D^*_{pg}(\text{from 7i})}\right| \times 100. \qquad (22)$$

If the percentage difference is less than 10% then proceed to the next step (7.k.). Otherwise repeat steps 7.f through 7.i using D^*_{pg} computed in 7.i. as the initial estimate in step 7.f. Continue this iterative process until the percent difference

is less than 10%.

k. Compute the Shape Factor, K_s, for the pile group (which is a function of the skew angle, α) using the following equation:

$$K_s \equiv \begin{cases} 1.0 & \text{for circular individual piles} \\ 0.9 + 0.66 \left| \alpha - \frac{\pi}{4} \right|^4 & \text{for square piles} \end{cases} . \quad (22)$$

l. Knowing D^*_{pg}, D_{50}, y_3, V_3, V_c, and K_s, the scour depth created by the pile group, $y_{s\,(pg)}$, can be estimated using single pile, equilibrium scour depth equations such as those given in Appendix B. Note that the structure shape factor is used in the scour depth calculation.

8. Compute the **Total Scour Depth for the Complex Pier**

The total estimated local scour depth at the complex pier is then the sum of the scour depths produced by the components of the pier,

$$y_s = y_{s\,(col)} + y_{s\,(pc)} + y_{s\,(pg)} \quad (23)$$

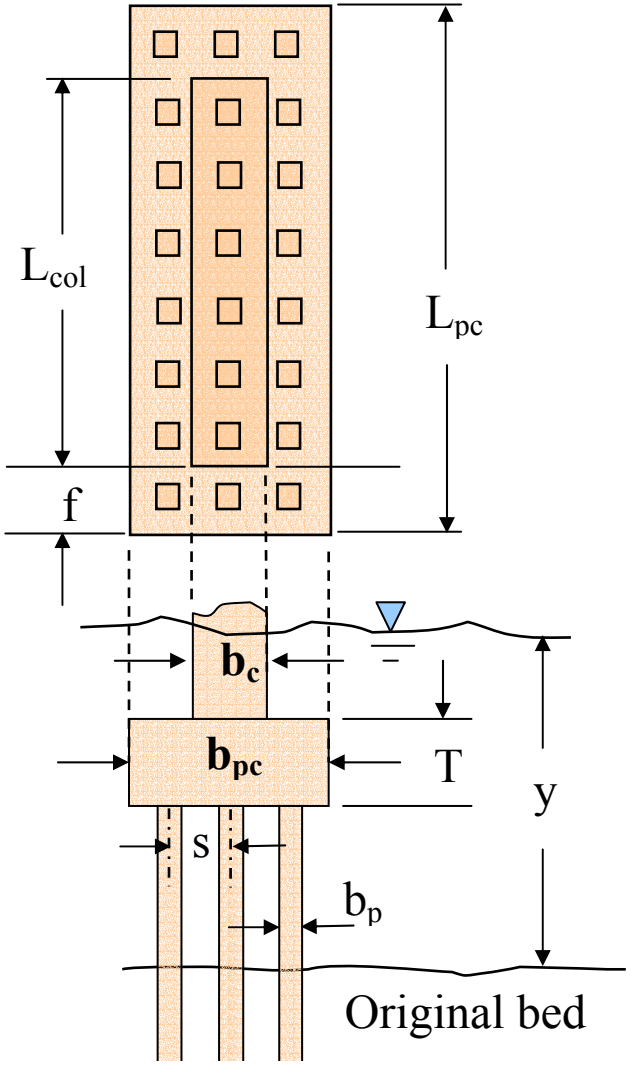

The piles in the pile group are in rows and columns when viewed from above. The rows are normal to the unskewed flow and the columns are parallel to the flow. The number of piles in a row (i.e. the number of piles normal to the unskewed flow) is denoted by, n, and the number in the column by, m. In

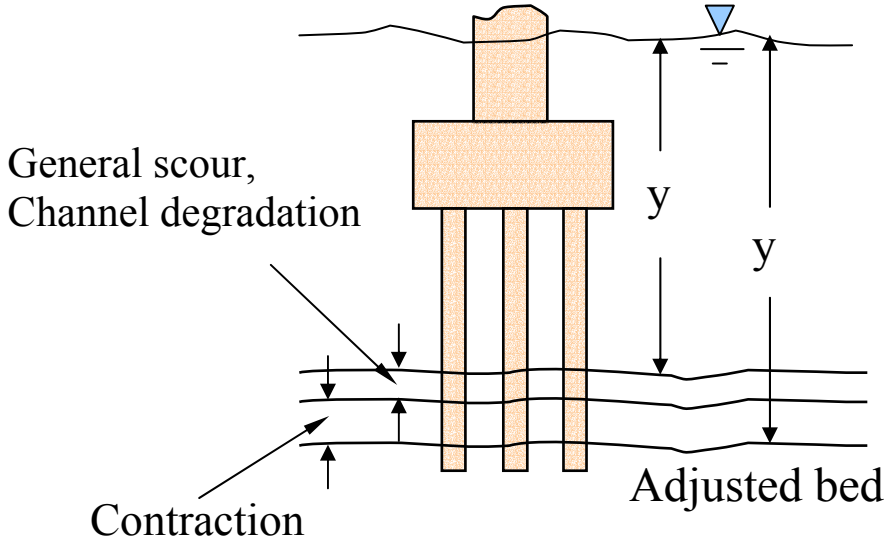

Figure 1. Complex Pier definition sketch showing bed adjusted for long-term scour, channel degradation and contraction scour.

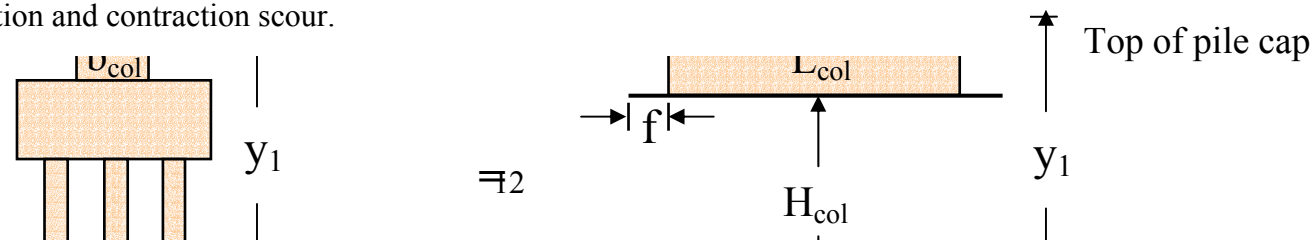

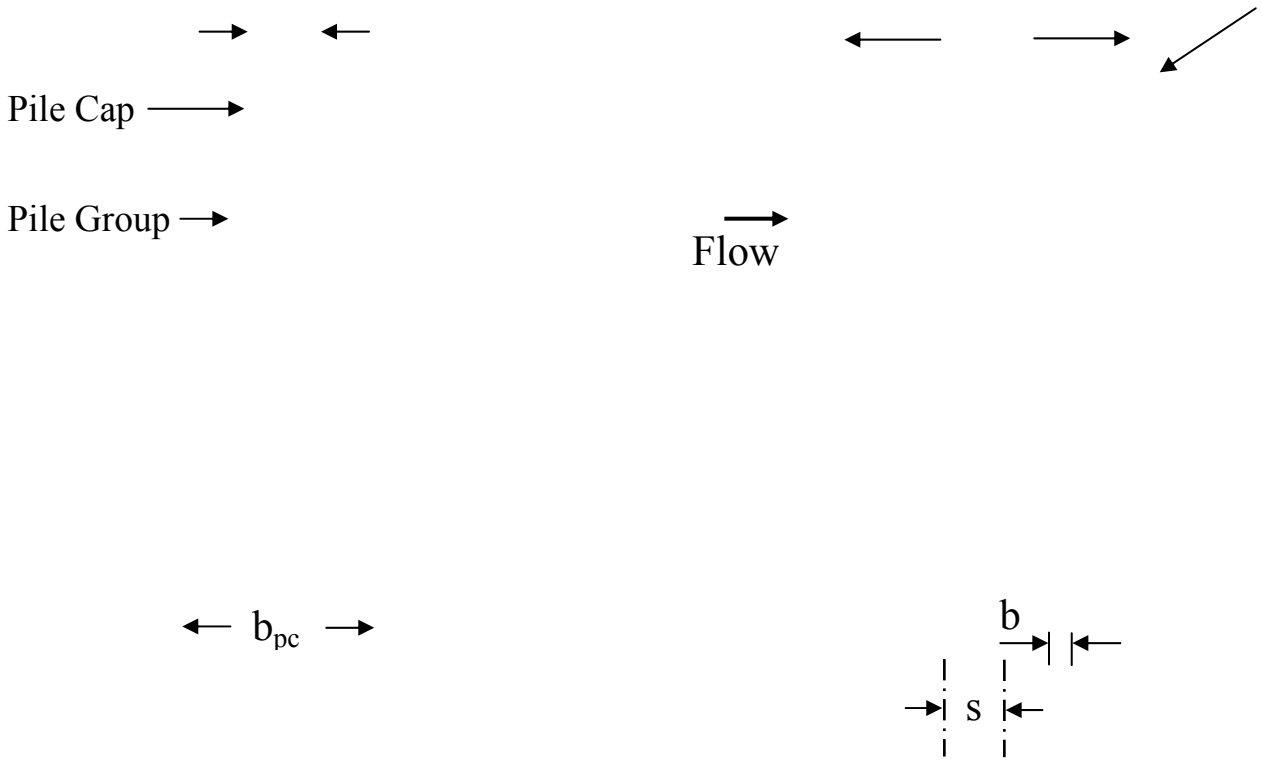

Figure 2. Complex Pier divided into its components, column, pile cap and pile group. The adjustment of the bed elevation for the scour due to the components

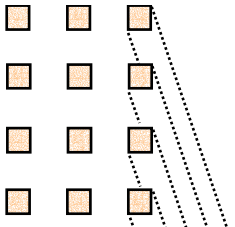

The projected width of the pile group, Wp, is obtained by summing the unobstructed projections of the piles in the first two rows and the first column onto a vertical plane that is normal to the flow. For the 3 x 8 pile group shown in the figure Wp = $l_1 + l_2 + l_3$.

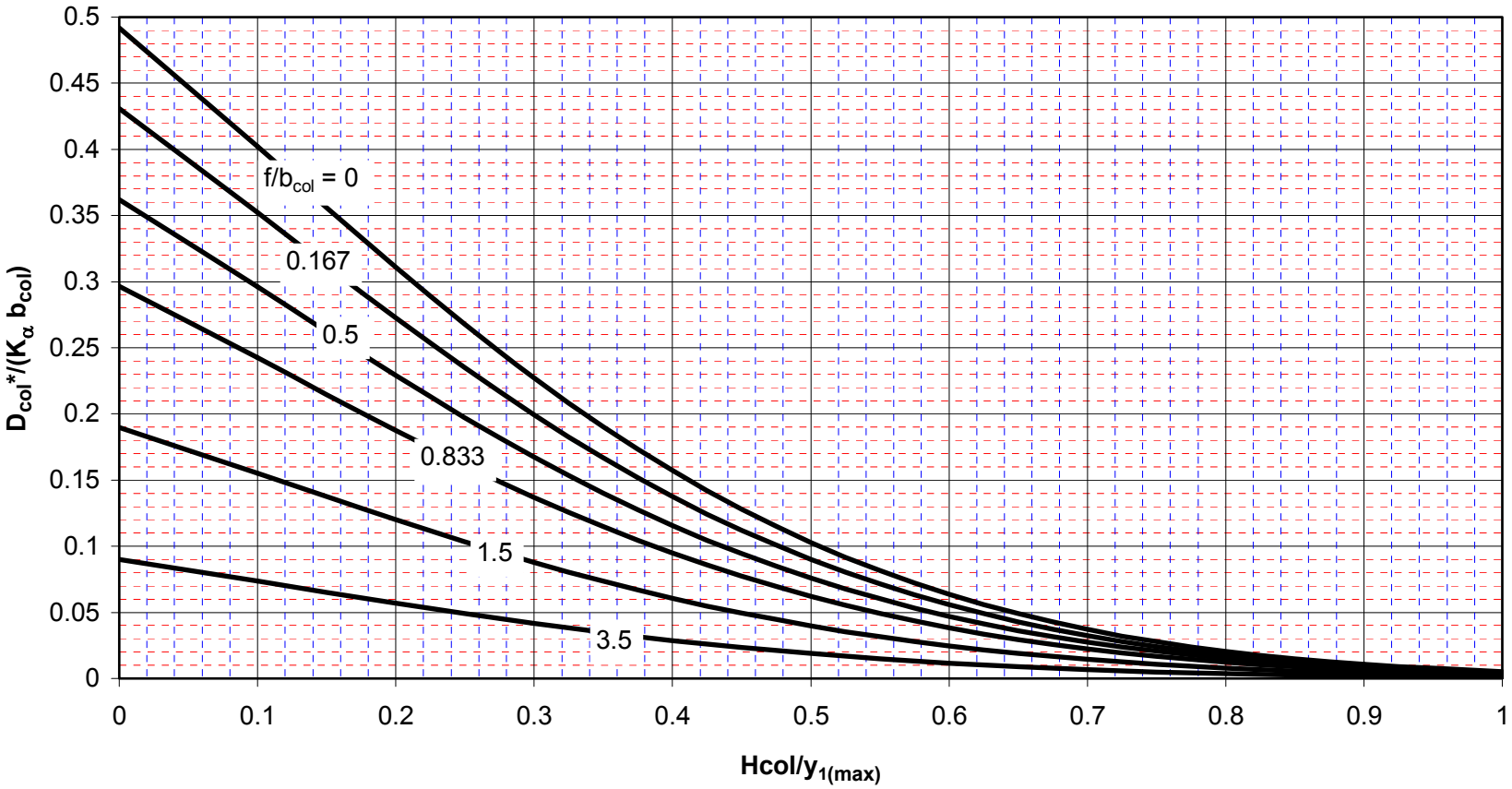

Figure 4. Effective diameter of the pile column, D_{col}*, as a function of the height of the column above the adjusted bed, H_{col}, and the pile cap extension in front of the column, f.

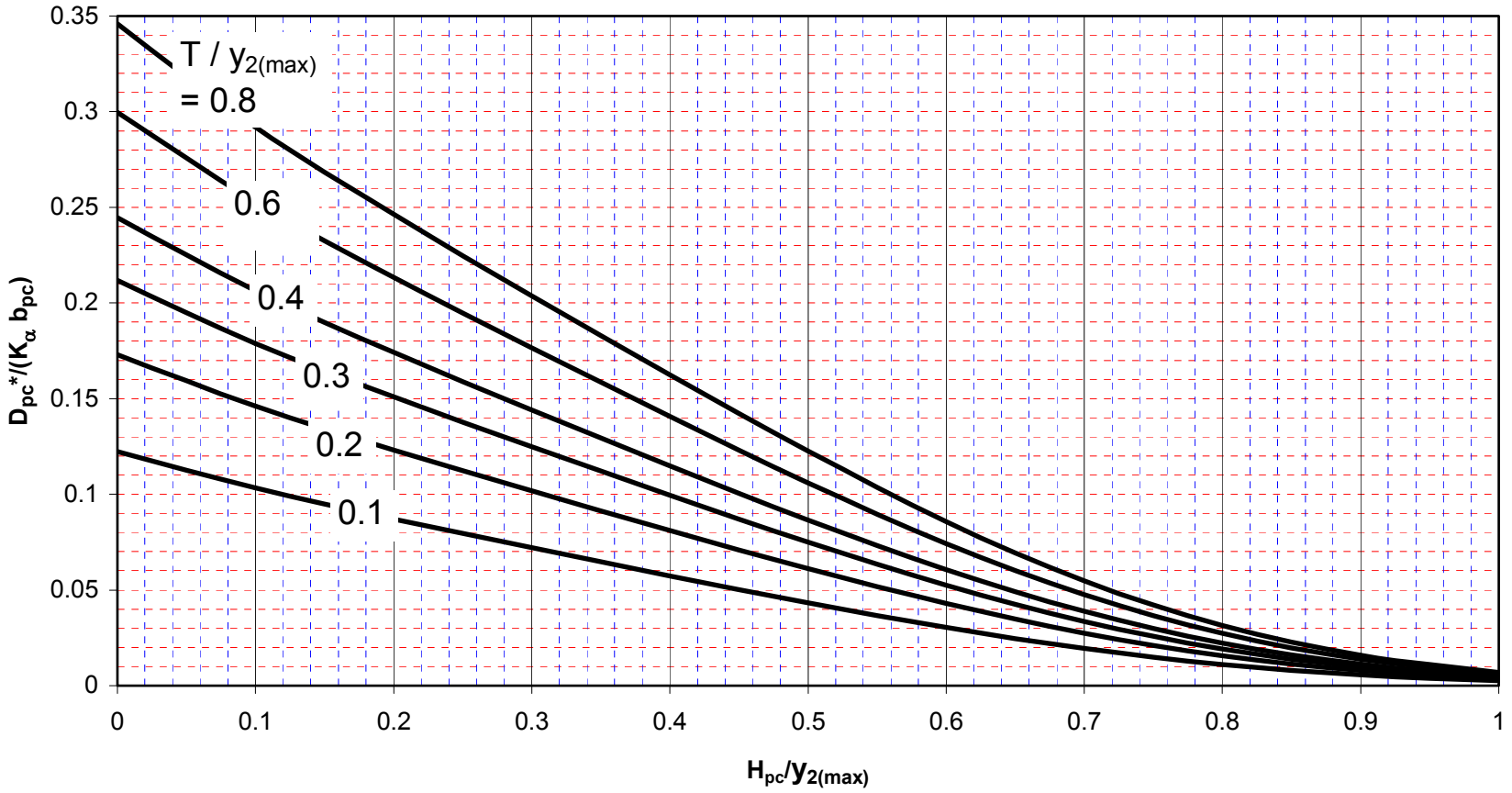

Figure 5. Effective diameter of the pile cap, D_{pc}*, as a function of the height of the bottom of the pile cap above the adjusted bed and the thickness of the pile cap, T.

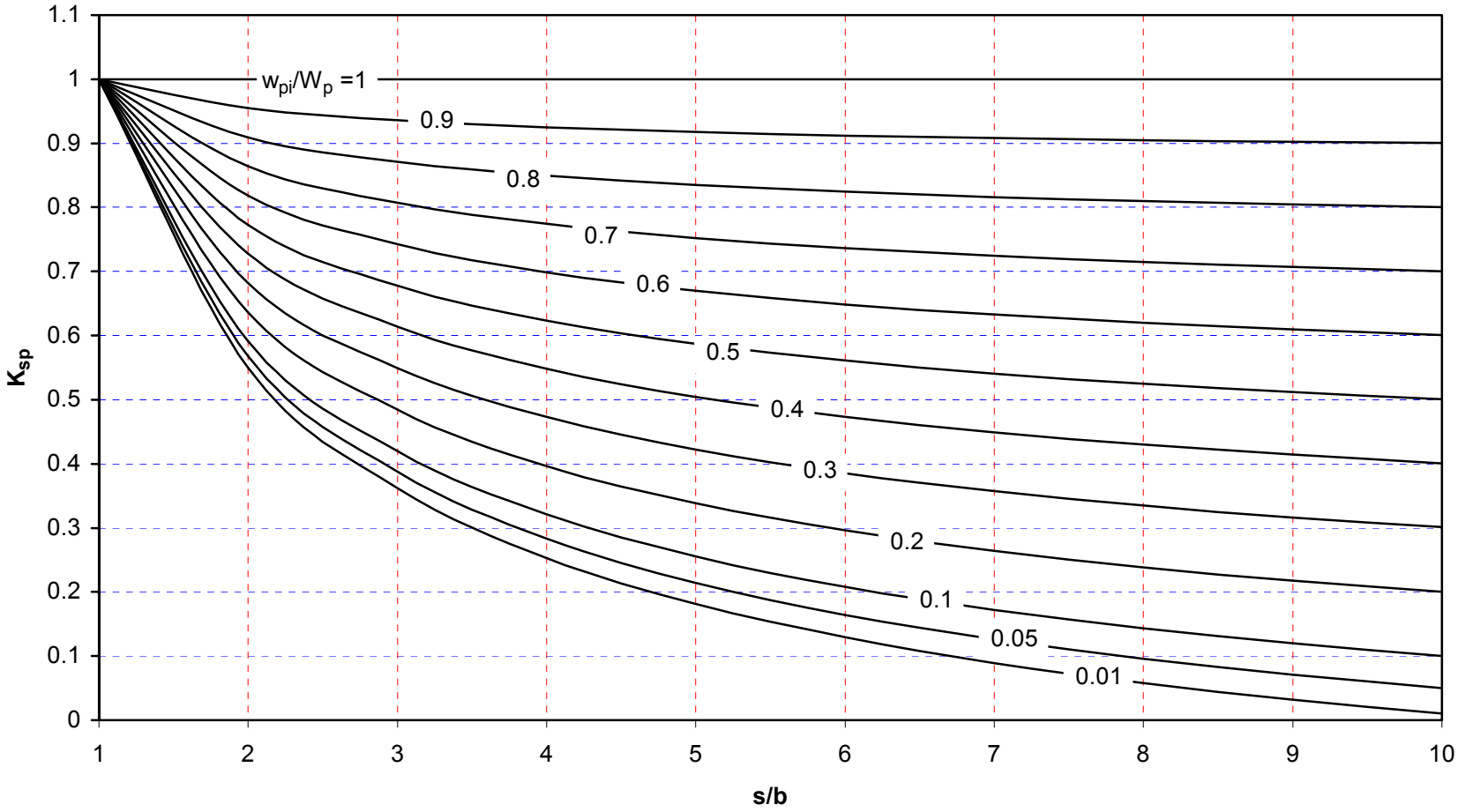

Figure 6. Pile spacing coefficient, K_{sp} as a function of the pile centerline spacing, s, and the projected width of a single, unobstructed pile in the group, w_{pi}.

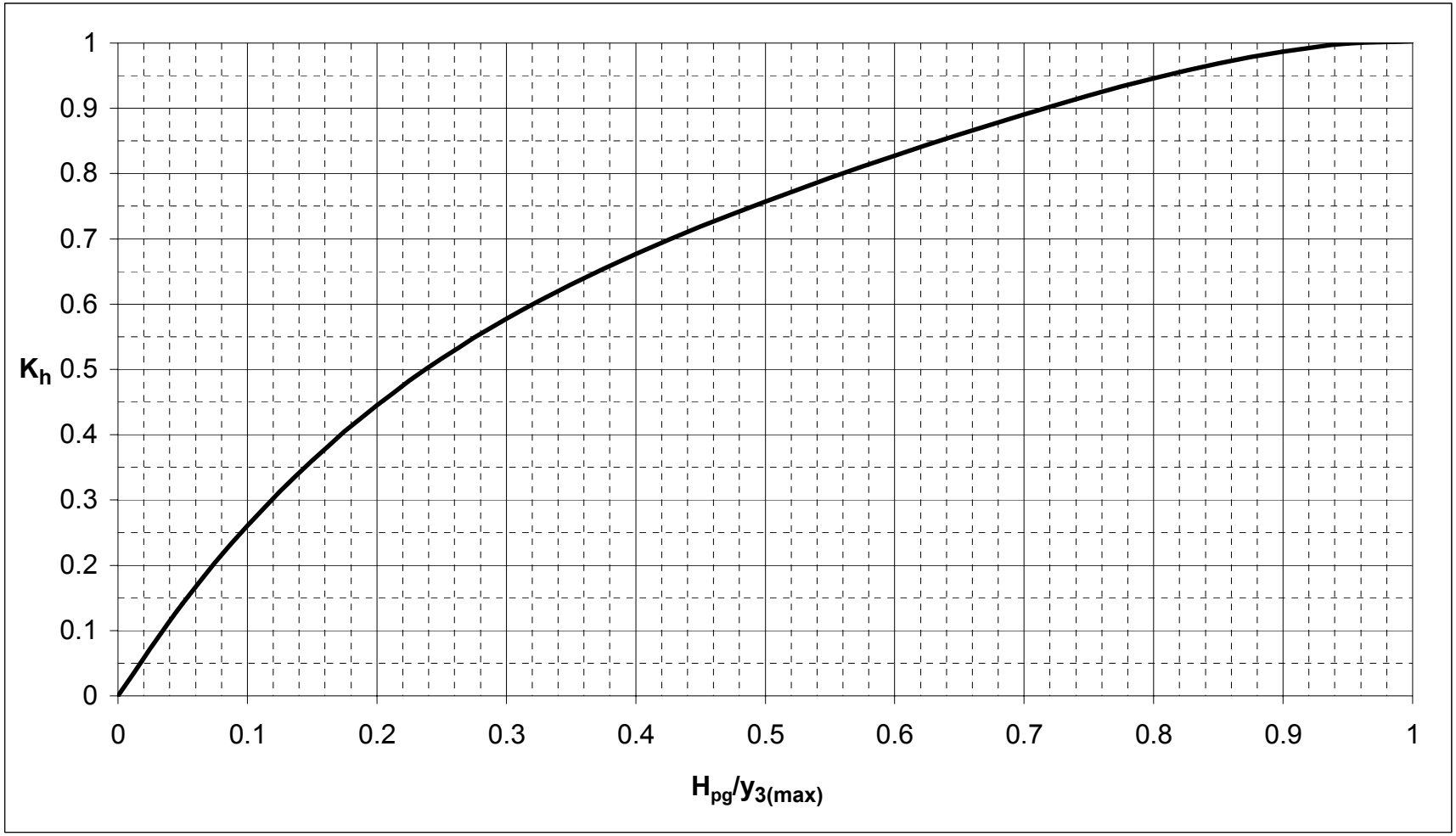

Figure 7. Pile group submergence coefficient, K_h, as a function of the height of the top of the piles above the adjusted bed.

Bibliography

Ahmad, M. (1953) "Experiments on Design and Behavior of Spur Dikes." *Proceedings of International Hydraulics Convention*, St. Anthony Falls Hydraulic Laboratory, Minneapolis, MN, 145-159.

Ahmad, M. (1962) "Discussion of 'Scour at Bridge Crossings' by E.M. Laursen." *Trans. of ASCE*, 127, pt. I(3294), 198-206.

Baker, R.E. (1986) "Local Scour at Bridge Piers in Non-uniform Sediment." Report No. 402, Department of Civil Engineering, University of Auckland, Auckland, New Zealand.

Basak V. (1975) "Scour at Square Piers." Devlet su isteri genel mudulugu, Report No. 583, Ankara, Turkey.

Blench, T. (1962) "Discussion of 'Scour at bridge crossings' by E.M. Laursen." *Trans. of ASCE*, 127, pt. I(3294), 180-183.

Bonasoundas M. (1973) "Non-stationary Hydromorphological Phenomena and Modelling of Scour Process." *Proc. 16th IAHR Congress*, Vol. 2, Sao Paulo, Brazil, 9-16.

Breusers, H.N.C., Nicollet, G. and Shen, H.W. (1977) "Local Scour Around Cylindrical piers." *Journal of Hydraulic Research*, 15(3), 211-252.

Chabert, J., and Engeldinger, P. (1956) "Etude des affouillements autour des piles des ponts." Laboratoire National d'Hydraulique, Chatou, France.

Chiew, Y.M. (1984) "Local scour at bridge piers." Master's Thesis, Auckland University, Auckland, New Zealand.

Chitale, S.V. (1962) "Discussion of 'Scour at bridge crossings' by E.M. Laursen." *Trans. of ASCE*, 127, pt. I(3294), 191-196.

Cunha, L.V. (1970) "Discussion of 'Local scour at bridge crossings' by Shen H.W., Schneider V.R. and Karaki S.S." *Trans. of ASCE*, 96(HY8), 191-196.

Ettema, R. (1976) "Influence of material gradation on local scour." Master's Thesis, Auckland University, Auckland, New Zealand.

Ettema, R. (1980) "Scour at bridge piers." PhD Thesis, Auckland University, Auckland, New Zealand.

Froehlich, D.C. (1988) "Analysis of on-site measurements of scour at piers." *Proc. of the 1988 National Conference on Hydraulic Engineering*, ASCE, New York, 534-539.

Gao Dong Guang, Posada, G., and Nordin C.F. (1992) "Pier scour equations used in the People's Republic of China." Draft, Department of Civil Engineering, Colorado State University, Fort Collins, CO.

Garde, R.J, Ranga Raju, K.G., and Kothyari, U.C. (1993) *Effect on unsteadiness and stratification on local scour*. International Science Publisher, New York.

Graf, W.H. (1995) "Local scour around piers." Annu. Rep., Laboratoire de Recherches Hydrauliques, Ecole Polytechnique Federale de Lausanne, Lausanne, Switzerland.

Hancu, S. (1971) "Sur le calcul des affouillements locaux dams la zone des piles de ponts." *Proc. 14th IAHR Congress*, Vol. 3, Paris, France, 299-313.

Hanna, C.R. (1978) "Scour at pile groups." Master of Engineering Thesis, University of Cantebury, Christchurch, New Zealand.

http://vortex.spd.louisville.edu/BridgeScour/whatis.htm (1998) "What is Bridge Scour?" Department of Civil Engineering, University of Louisville.

Inglis, S.C. (1949) "The behavior and control of rivers and canals." Central Water Power Irrigation and Navigation Report, Publication 13, part II, Poona Research Station, Poona, India.

Jain, S.C., and Fischer, E.E. (1979) "Scour around circular bridge piers at high Froude numbers." Rep. No. FHWA-RD-79-104, FHWA, Washington DC.

Jette, C.D., and Hanes, D.M. (1997) "High resolution sea-bed imaging: an acoustic multiple transducerarray." *Measurement Science and Technology*, 8, 787-792.

Jones, J. Sterling and D. Max Sheppard. (2000) "Scour at Wide Piers," Proceedings for the 2000 Joint Conference on Water Resources Engineering and Water Resources Planning and Management Conference, Minneapolis, MN, July 30-August 2, 2000.

Krishnamurthy, M. (1970) "Discussion of 'Local scour at bridge crossings' by Shen H.W., Schneider V.R. and Karaki S.S." *Trans. of ASCE*, 96(HY7), 1637-1638.

Larras, J. (1963) "Profondeurs Maximales d'Erosion des Fonds Mobiles autour des Piles en Riviere." Annales des Ponts et Chausses, Vol. 133, No. 4, 424-441.

Laursen E.M. (1962) "Scour at bridge crossings." *Trans. of ASCE*, 84(HY1), 166-209.

Laursen, E.M. (1958) "Scour at Bridge Crossings." Iowa Highway Research Bd., Bulletin No. 8.

Laursen E.M., and Toch A. (1956) "Scour around bridge piers and abutments." Bulletin No. 4, Iowa Highway Research Board, Ames, IA.

Melville, B.W. (1975) "Local scour at bridge sites." Report no. 117, University of Auckland, School of Engineering, Auckland, New Zealand.

Melville, B.W. (1984) "Live Bed Scour at Bridge Piers." J. Hydraulic Engineering, Vol. 110, No. 9, pp 1234-1247.

Melville, B.W. (1997) "Pier and abutment scour-an integrated approach." *Journal of Hydraulic Engineering*, 123(2), 125-136.

Melville, B.W., and Chiew, Y.M. (1999) "Time scale for local scour at bridge piers." *Journal of Hydraulic Engineering*, 125(1), 59-65.

Melville, B.W., and Sutherland, A.J. (1988) "Design method for local scour at bridge piers." *Journal of Hydraulic Engineering*, 114(10), 1210-1226.

Neill, C.R. (1964) "River bed scour, a review for bridge engineers." Contract No. 281, Res. Council of Alberta, Calgary, Alberta, Canada.

Neill, C.R. (1973) *Guide to Bridge Hydraulics*. Roads and Transportation Association of Canada, University of Toronto Press, Canada.

Nicollet, G., and Ramette, M. (1971) "Affouillement au voisinage de pont cylindriques circularies" *Proc. of the 14th IAHR Congress*, Vol. 3, Paris, France, 315-322.

Pilarczyk, K.W. (1995) "Design tools related to revetments including riprap." *River, coastal and shoreline protection: Erosion control using riprap and armour stone*, John Wiley & Sons, New York, 17-38.

Raudkivi, A.J., and Ettema, R. (1977) "Effect of sediment gradation on clear water scour." *Journal of Hydraulic Engineering*, 103(10), 1209-1212.

Rouse, H. (1946) *Elementary Fluid Mechanics*. John Wiley & Sons, New York.

Shen, H.W. (1971) "Scour near piers." *River Mechanics*, Vol. II, Chapter 23, Colorado State University, Fort Collins, CO.

Shen, H.W., Schneider, V.R. and Karaki, S.S. (1969) "Local Scour around Bridge Piers." Proc. ASCE, J. Hydraulics Div., Vol. 95, No. HY6.

Shen, H.W., Schneider, V.R. and Karaki, S.S. (1966) "Mechanics of Local Scour." Colorado State University, Civil Engineering Dept., Fort Collins, Colorado, Pub. No. CER66-HWS22.

Sheppard, D. Max, Jeffrey Sheldon, Eric Smith, and Mufeed Odeh. (2000) "Hydraulic Modeling and Scour Analysis for the San Francisco-Oakland Bay Bridge," Proceedings for the 2000 Joint Conference on Water Resources Engineering and Water Resources Planning and Management Conference, Minneapolis, MN, July 30-August 2, 2000.

Sheppard, D. Max, Mufeed Odeh, Tom Glasser, and Athanasios Pritsivelis. (2000) "Clearwater Local Scour Experiments with Large Circular Piles," Proceedings for the 2000 Joint Conference on Water Resources Engineering and Water Resources Planning and Management Conference, Minneapolis, MN, July 30-August 2, 2000.

Sheppard, D. Max, Mufeed Odeh, Athanasios Pritsivelis, and Tom Glasser. (2000) "Clearwater Local Scour Experiments in a Large Flume." Proceedings for the 2000 Joint Conference on Water Resources Engineering and Water Resources Planning and Management Conference, Minneapolis, MN, July 30-August 2, 2000.

Sheppard, D. Max. (2001) " A Methodology for Estimating Local Scour Depths at Bridge Piers with Complex Geometries," In Preparation.

Sheppard, D. Max. (2000) "A Method for Scaling Local Sediment Scour Depths from

Model to Prototype," Proceedings for the 2000 Joint Conference on Water Resources Engineering and Water Resources Planning and Management Conference, Minneapolis, MN, July 30-August 2, 2000.

Sheppard, D. Max. (2000) "Physical Model Local Scour Studies of the Woodrow Wilson Bridge Piers," Proceedings for the 2000 Joint Conference on Water Resources Engineering and Water Resources Planning and Management Conference, Minneapolis, MN, July 30-August 2, 2000.

Sheppard, D. Max, and Sterling Jones. (2000) "Local Scour at Complex Piers," Proceedings for the 2000 Joint Conference on Water Resources Engineering and Water Resources Planning and Management Conference, Minneapolis, MN, July 30-August 2, 2000.

Sheppard, D.M. (1997) "Conditions of maximum local scour." Report No. UFL/COEL-97/006, Coastal and Oceanographic Engineering Department, University of Florida, Gainesville, FL.

Sheppard, D.M., and Jones, J.S. (1998) "Scour at complex pier geometries." *Compendium of scour papers from ASCE Water Resources Conferences*, Eds. E.V. Richardson and P.F. Lagasse, ASCE, New York.

Sheppard, D.M., and Ontowirjo, B. (1994) "A local sediment scour prediction equation for circular piles." Report No. UFL/COEL-TR/101, Coastal and Oceanographic Engineering Department, University of Florida, Gainesville, FL.

Sheppard, D.M., Zhao, G., and Ontowirjo, B. (1999) "Local Scour Near Single Piles in Steady Currents." Stream Stability and Scour At Highway Bridges, Compendium of Papers, *ASCE Water Resources Engineering Conferences 1991 to 1998,* Edited by E.V. Richardson and P.F. Lagasse.

Sheppard, D.M., Zhao, G., and Ontowirjo, B. (1995) "Local scour near single piles in steady currents." *ASCE Conference Proceedings: The First International Conference on Water Resources Engineering*, San Antonio, TX.

Shields, A. (1936) "Anwendung der Aehnlichkeitsmechanik und der turbulenz forschung auf die geschiebebewegung." Mitt. Preuss. Versuchanstalt Wesserbau Schiffbau, Berlin, Germany.

Sleath, J.F. (1984) *Sea Bed Mechanics*. John Wiley & Sons, New York.

Snamenskaya, N.S. (1969) "Morphological principle of modelling of river-bed processes." *Science Council of Japan*, vol. 5-1, Tokyo, Japan.

Tison, L.J. (1940) "Erosion autour des piles de ponts en riviere." *Annales des Travaux Publics de Belgique*, 41(6), 813-817.

U.S. Department of Transportation (1995) "Evaluating scour at bridges." Hydraulic Engineering Circular No. 18, Pub. No. FHWA-IP-90-017. FHWA, Washington DC.

van Rijn, Leo C. (1993) “Principles of Sediment Transport in Rivers, Estuaries and Coastal Seas,” Aqua Publications, PO Box 9896, 1006 AN Amsterdam, The Neatherlands.

Venkatadri, C. (1965) “Scour around bridge piers and abutments.” *Irrigation Power*, January, 35-42.

White W. R. (1973) “Scour around bridge piers in steep streams.” *Proc. 16th IAHR Congress*, Vol. 2, Sao Paulo, Brazil, 279-284.

APPENDIX A
EXPERIMENTAL DATA

The data presented in this appendix was obtained in several laboratories as discussed in the main report. The symbols in the tables are defined in Figure A1 and in the List of Symbols in the main report. In order to account for the impact of the pile cap on the scour produced by the column a thin plate was attached to the bottom of the column with varying protrusions lengths (f). The pile caps in the "pile cap alone" experiments were supported by small rods from above. These configurations are shown schematically in Figure A1 below.

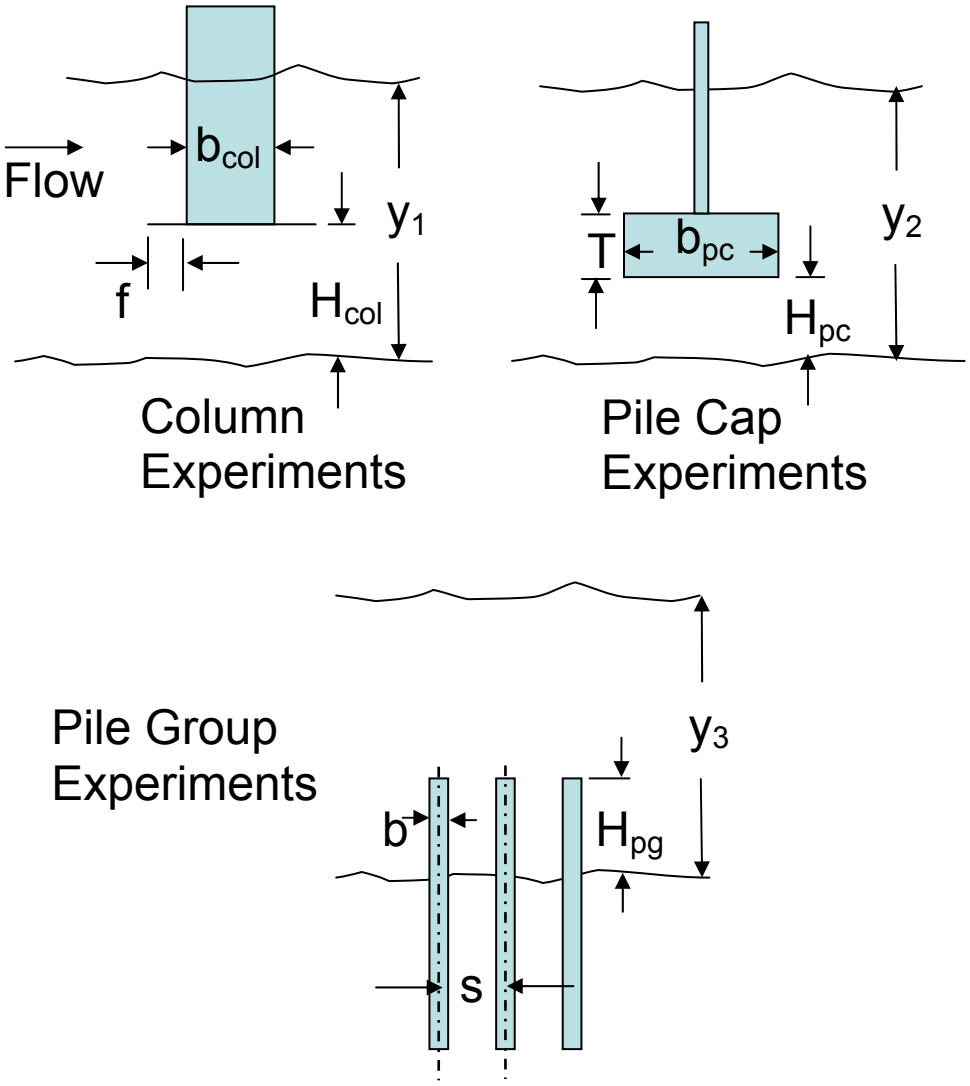

Figure A1. Schematic drawings of experimental setups and symbols used in the following tables.

EXPERIMENTAL DATA

Table A1. Data for Column Only experiments. Data obtained by Sterling Jones at FHWA.

RUN No.	y_0 (m)	D_{50} (mm)	V (m/s)	V_C (m/s)	V/V_c	H_{col} (m)	b_{col} (m)	f (m)	f/b_{col}
67	0.305	1	0.41	0.44	0.95	-0.30	0.1524	0	0.000
63	0.305	1	0.40	0.44	0.92	-0.24	0.1524	0	0.000
64	0.305	1	0.41	0.44	0.94	-0.18	0.1524	0	0.000
65	0.305	1	0.42	0.44	0.96	-0.12	0.1524	0	0.000
66	0.305	1	0.41	0.44	0.94	-0.06	0.1524	0	0.000
68	0.305	1	0.41	0.44	0.95	0.00	0.1524	0	0.000
69	0.305	1	0.42	0.44	0.95	0.06	0.1524	0	0.000
70	0.305	1	0.41	0.44	0.93	0.12	0.1524	0	0.000
71	0.305	1	0.41	0.44	0.94	0.18	0.1524	0	0.000
72	0.305	1	0.40	0.44	0.92	0.24	0.1524	0	0.000
73	0.305	1	0.42	0.44	0.97	0.00	0.0762	0.1143	1.500
74	0.305	1	0.42	0.44	0.96	0.06	0.0762	0.1143	1.500
81	0.305	1	0.42	0.44	0.96	0.00	0.1524	0.0762	0.500
83	0.305	1	0.43	0.44	0.99	0.06	0.1524	0.0762	0.500
84	0.305	1	0.41	0.44	0.95	0.12	0.1524	0.0762	0.500
85	0.305	1	0.42	0.44	0.97	0.18	0.1524	0.0762	0.500
75	0.305	1	0.41	0.44	0.94	0.00	0.2286	0.0381	0.167
76	0.305	1	0.43	0.44	0.97	0.06	0.2286	0.0381	0.167
77	0.305	1	0.42	0.44	0.95	0.12	0.2286	0.0381	0.167
79	0.305	1	0.42	0.44	0.96	0.18	0.2286	0.0381	0.167
80	0.305	1	0.42	0.44	0.97	0.24	0.2286	0.0381	0.167
95	0.305	1	0.42	0.44	0.95	0.00	0.0762	0.2667	3.500
96	0.305	1	0.42	0.44	0.96	0.06	0.0762	0.2667	3.500
91	0.305	1	0.42	0.44	0.95	0.00	0.1524	0.2286	1.500
92	0.305	1	0.42	0.44	0.95	0.06	0.1524	0.2286	1.500
93	0.305	1	0.43	0.44	0.98	0.12	0.1524	0.2286	1.500
94	0.305	1	0.43	0.44	0.98	0.18	0.1524	0.2286	1.500
86	0.305	1	0.42	0.44	0.96	0.00	0.2286	0.1905	0.833
87	0.305	1	0.43	0.44	0.98	0.06	0.2286	0.1905	0.833
88	0.305	1	0.42	0.44	0.96	0.12	0.2286	0.1905	0.833
89	0.305	1	0.41	0.44	0.94	0.18	0.2286	0.1905	0.833
90	0.305	1	0.42	0.44	0.96	0.24	0.2286	0.1905	0.833

Table A2. Data for Pile Cap Only experiments. Data obtained by D. Max Sheppard at the University of Florida and Sterling Jones at FHWA.

Run No.	y_0 (m)	D_{50} (mm)	V (m/s)	V_C (m/s)	V/V_c	T (m)	H_{pc} (m)	b_{pc} (m)	y_s Measured (m)
1	0.305	1	0.43	0.44	0.97	0.030	0	0.305	0.1006
58	0.305	1	0.39	0.44	0.90	0.030	0.091	0.305	0.0347
59	0.305	1	0.41	0.44	0.94	0.030	0.152	0.305	0.0189
61	0.305	1	0.41	0.44	0.95	0.030	0.183	0.305	0.0134
5	0.305	1	0.42	0.44	0.96	0.030	0.244	0.305	0.0146
6	0.305	1	0.42	0.44	0.96	0.030	0.274	0.305	0.0018
7	0.305	1	0.42	0.44	0.95	0.061	0	0.305	0.1317
12	0.305	1	0.42	0.44	0.96	0.061	0.091	0.305	0.0671
10	0.305	1	0.42	0.44	0.97	0.061	0.091	0.305	0.0677
8	0.305	1	0.42	0.44	0.96	0.061	0.152	0.305	0.0408
9	0.305	1	0.42	0.44	0.95	0.061	0.183	0.305	0.0268
11	0.305	1	0.42	0.44	0.96	0.061	0.244	0.305	0.0165
13	0.305	1	0.42	0.44	0.96	0.061	0.274	0.305	0.0067
*14	0.305	1	0.42	0.44	0.95	0.091	0	0.305	0.1412
15	0.305	1	0.42	0.44	0.96	0.091	0.091	0.305	0.0817
16	0.305	1	0.41	0.44	0.93	0.091	0.152	0.305	0.0543
17	0.305	1	0.42	0.44	0.95	0.091	0.183	0.305	0.0634
18	0.305	1	0.43	0.44	0.97	0.091	0.244	0.305	0.0317
19	0.305	1	0.43	0.44	0.97	0.122	0	0.305	0.1750
20	0.305	1	0.42	0.44	0.97	0.122	0.091	0.305	0.1018
21	0.305	1	0.42	0.44	0.96	0.122	0.152	0.305	0.0701
22	0.305	1	0.42	0.44	0.97	0.122	0.183	0.305	0.0792
11	0.305	1	0.42	0.44	0.96	0.122	0.244	0.305	0.0165
6	0.305	1	0.42	0.44	0.96	0.122	0.274	0.305	0.0018
A	0.305	0.18	0.27	0.27	0.99	0.183	0.183	0.305	0.0556
B	0.305	0.18	0.25	0.27	0.92	0.183	0.122	0.305	0.0730
C	0.305	0.18	0.25	0.27	0.92	0.183	0	0.305	0.1270
D	0.305	0.18	0.25	0.27	0.92	0.244	0.122	0.305	0.0762
E	0.305	0.18	0.25	0.27	0.92	0.244	0.061	0.305	0.1333
F	0.305	0.18	0.25	0.27	0.92	0.244	0	0.305	0.1730

Table A3. Data for Pile Groups Only experiments. Data obtained by D. Max Sheppard at the University of Florida and Conte USGS Laboratory.

RUN No.	y_0 (m)	D_{50} (mm)	V_C (m/s)	V (m/s)	V/V_c	H_{pg} (m)	α	n	m	b (m)	s/b	y_s Measured (m)
1	0.356	0.172	0.28	0.23	0.83	0.089	90	8	3	0.03175	3	0.076
2	0.356	0.172	0.28	0.23	0.82	0.089	0	3	8	0.03175	3	0.069
3	0.368	0.172	0.28	0.23	0.84	0.184	90	8	3	0.03175	3	0.114
4	0.375	0.172	0.28	0.23	0.85	0.187	0	3	8	0.03175	3	0.097
5	0.391	0.189	0.28	0.23	0.80	0.294	90	8	3	0.03175	3	0.146
6	0.373	0.189	0.28	0.25	0.89	0.279	0	3	8	0.03175	3	0.102
7	0.381	0.172	0.28	0.24	0.87	0.381	0	3	8	0.03175	3	0.132
8	1.201	0.22	0.32	0.33	1.03	1.201	90	8	3	0.03175	3	0.241
9	1.199	0.22	0.32	0.30	0.96	1.198	70	3	8	0.03175	3	0.380
10	0.381	0.172	0.28	0.23	0.81	0.381	0	2	4	0.03175	6	0.085
11	0.381	0.172	0.26	0.23	0.88	0.381	0	3	1	0.03175	3	0.089
12	0.381	0.172	0.27	0.28	1.04	0.381	0	3	3	0.03175	3	0.122
13	0.378	0.172	0.27	0.23	0.87	0.381	0	3	5	0.03175	3	0.1143

Table A4. Data for Pile Group Submergence Only experiments. Data obtained by D. Max Sheppard at the University of Florida.

Test No.	n	m	H_{pg}/y_o	Water Depth, y_0 (m)	Wp (m)	b/Wp	$H_{pg\ (m)}$	Sediment Diameter, D_{50} (mm)	V/V_c	D* (m)
1	8	3	¼	0.356	0.254	0.125	0.09	0.172	0.803	0.08
2	3	8	¼	0.356	0.095	0.333	0.09	0.172	0.793	0.07
3	8	3	½	0.368	0.254	0.125	0.18	0.172	0.811	0.15
4	3	8	½	0.375	0.095	0.333	0.19	0.172	0.820	0.11
5	8	3	¾	0.392	0.254	0.125	0.29	0.189	0.781	0.25
6	3	8	¾	0.373	0.095	0.333	0.28	0.189	0.859	0.10

APPENDIX B
EQUILIBRIUM LOCAL SCOUR DEPTHS AT SINGLE PILES

EQUILIBRIUM LOCAL SCOUR DEPTHS AT SINGLE PILES

INTRODUCTION

The equations and methods for computing equilibrium local scour depths at circular piles discussed in this appendix are the most recent version of those originally proposed by Sheppard et al. (1995). The equations presented here have been improved over the original version as new data was obtained.

Equilibrium local scour depth at a single circular pile can be computed as follows (refer to the Figures B1 and B2). For design purposes, local scour depth is computed using equations that plot as shown in the schematic drawing of $\frac{y_s}{b}$ vs. $\frac{V}{V_c}$ in Figure B2. If the velocity where the scour depth is desired is in the clearwater scour range (i.e. $0.47 \le \frac{V}{V_c} \le 1.0$) the scour is computed using the equation for the curve between points 1 and 2 in the sketch. For velocities in the live bed scour range $1.0 < \frac{V}{V_c} \le \frac{V_{lp}}{V_c}$, (where V_{lp} is the velocity at the live bed peak scour depth) the equation for the line between points 2 and 3 is used. For $\frac{V}{V_c} > \frac{V_{lp}}{V_c}$, the dimensionless scour depth remains constant at the value at point 3.

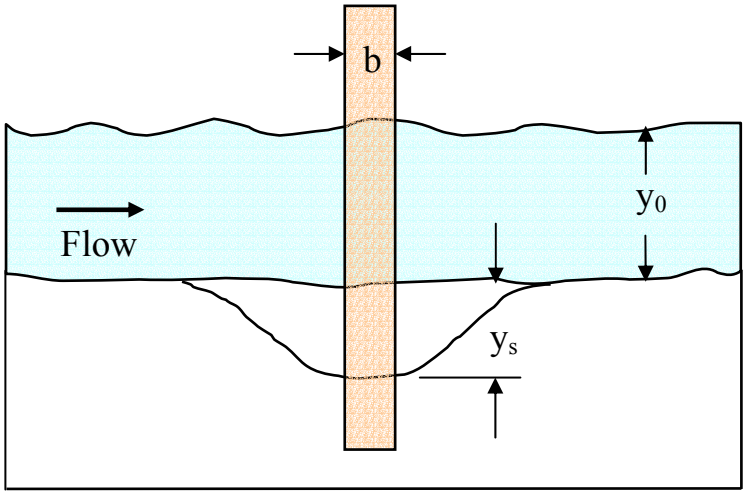

Figure B1. Definition sketch of local scour at a circular pile.

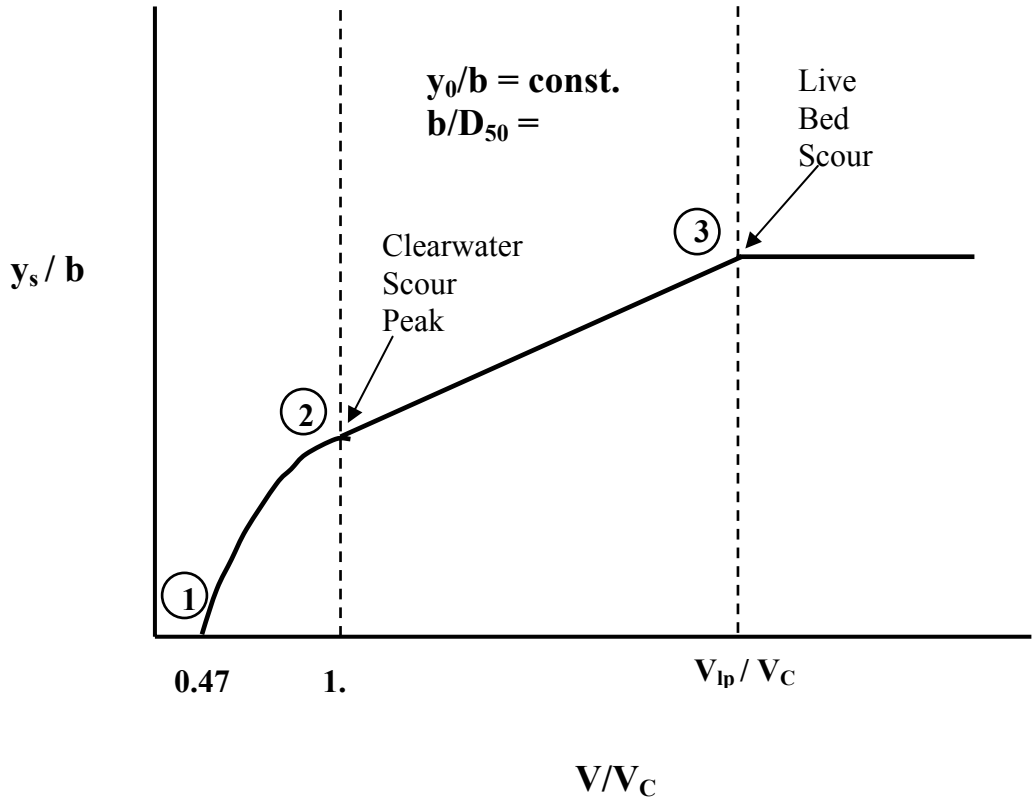

Figure B2. Definition sketch. Normalized equilibrium, local scour depth versus normalized depth averaged velocity.

The critical depth averaged velocity, V_c, must be obtained first. Knowing the median sediment size, D_{50}, sediment specific gravity, sg, water depth, y_0, and relative roughness of the bed, RR, the critical velocity can be computed using equations presented near the end of this appendix or (for quartz sand) obtained from Figures B3 thru B5. These equations and curves are based on Shield's Diagram. Guidelines for the proper value of RR to use can be found in Table B1. For relatively smooth sandy bottom channels void of vegetation, a relative roughness of 10 to 15 would be appropriate. For vegetated channels or channels with oyster beds or rock outcroppings, larger values, on the order of 20 to 30 or even higher, should be used. The value of critical velocity is not very sensitive to relative roughness of the bed; thus, errors in estimating this value will not have a major impact on critical velocity predictions. Knowing the design and critical velocities, the scour regime can be determined (i.e. is the design velocity in the clearwater scour or the live bed scour regime).

Clearwater Scour Equations

Clearwater Scour $\left(0.47 \le \frac{V}{V_c} \le 1.0\right)$**:**

If the design velocity is in the clearwater scour range Equation 5 can be used to compute the scour depth.

$$\frac{y_s}{b} = 2.5\, K_S\, f_1\left(\frac{y_0}{b}\right) f_2\left(\frac{V}{V_c}\right) f_3\left(\frac{b}{D_{50}}\right), \tag{B1}$$

where

$$f_1\left(\frac{y_0}{b}\right) = tanh\left[\left(\frac{y_0}{b}\right)^{0.4}\right], \tag{B2}$$

$$f_2\left(\frac{V}{V_c}\right) = 1 - 1.75\left[ln\left(V/V_c\right)\right]^2$$

$$f_3\left(\frac{b}{D_{50}}\right) =$$

$$\frac{3.05}{2.6\, exp\left[0.45\left(log\left(\frac{b}{D_{50}}\right) - 1.64\right)\right] + 0.45\, exp\left[-2.6\left(log\left(\frac{b}{D_{50}}\right) - 1.64\right)\right]}, \tag{B3}$$

and

$K_s \equiv$ Shape factor (1 for circular piles). (B4)

$$\frac{y_s}{b} = 2.5\, K_s \left\{tanh\left[\left(\frac{y_0}{b}\right)^{0.4}\right]\right\} \left\{1 - 1.75\left[ln\left(V/V_c\right)\right]^2\right\}$$

$$\left\{\frac{3.05}{2.6\, exp\left[0.45\left(log\left(\frac{b}{D_{50}}\right) - 1.64\right)\right] + 0.45\, exp\left[-2.6\left(log\left(\frac{b}{D_{50}}\right) - 1.64\right)\right]}\right\}. \tag{B5}$$

If the design velocity is in the live bed regime, then the velocity where the maximum scour depth in the live bed range occurs (V_{lp}) (point 3 in Figure B2) must be determined.

The velocity at which the so called, "live bed peak" occurs is thought to be the velocity where the flat bed planes out (i.e. the velocity where the dunes are swept away and the bed becomes planer). Several publications in the literature give information about, and methods for, computing the conditions under which the bed planes out. The results presented by Snamenskaya (1969) and those by van Rijn (1993) yield plane bed velocities that are very close to each other. Van Rijn's method is easier to use and is thus the one recommended for use here.

In this method two conditions must be met. The velocity for each condition is computed and the larger of the two values used. Which of the two values is larger will depend on the sediment and water properties and the flow velocity and water depth. Van Rijn's method and equations are presented near the end of this appendix. Plots using Snamenskaya's results are presented in Figures B6 and B7.

Knowledge of the sediment size and size distribution, (D_{50} and D_{90}), water depth, and water and sediment densities are needed in order to determine $V_{lp.}$ If D_{90} is not known it can be approximated by the value for D_{50}. This will yield a more conservative estimate for the equilibrium scour depth (i.e. a greater local scour depth).

Live Bed Scour Equations

Live Bed Scour

If $\left(1.0 < \frac{V}{V_c} < \frac{V_{lp}}{V_c}\right)$

$$\frac{y_s}{b} = K_s \; f_1\left(\frac{y_0}{b}\right)\left[2.2\left(\frac{V - V_c}{V_{lp} - V_c}\right) + 2.5 \; f_2\left(\frac{b}{D_{50}}\right)\left(\frac{V_{lp} - V}{V_{lp} - V_c}\right)\right]. \quad \text{(B6)}$$

If $\frac{V}{V_c} > \frac{V_{lp}}{V_c}$

$$\frac{y_s}{D} = 2.2 \; K_s \; tanh\left[\left(\frac{y_0}{D}\right)^{0.4}\right] \quad \text{(B7)}$$

From the somewhat limited data in the literature for velocities near the live bed peak velocity the value of the constant, K_{lp} is approximately 2.2. Note that the scour depth at transition $\left(\frac{V}{V_c} = 1\right)$ must be computed as well as for the live bed design velocity since under some conditions, (small structures in large diameter sediment) the transition scour depth may be greater than that at the design velocity. The larger of the two values would be the correct one to use.

4.4 Local Scour Depths for Noncircular Piles

The scour depth for noncircular single piles can be computed by using the appropriate value for the shape factor K_s for the pile cross-sectional shape in Equations 5 - 7. Values for K_s from HEC-18 are reproduced in Table B2.

Table B1. Bed relative roughness, RR, guide.

Bed Condition	RR
Laboratory flume, smooth bed– ripple forming sand (D_{50} < 0.6 mm)	5.0
Laboratory flume, smooth bed – non-ripple forming sand (D_{50} > 0.6 mm)	2.5
Laboratory flume, smooth bed – live bed test with dunes	10
Field – smooth bed	10
Field – moderate bed roughness	15
Field – rough bed	20

Table B2. Single pile shape coefficients (information from HEC-18).

Pile Shape	**Shape Factor K_s (K_1 in HEC-18)**
Circular	1.0
Square Flow normal to side → ◇	0.9
Flow normal to edge → □	1.1

Critical Depth-Averaged Velocity

The critical bed shear stress and the associated critical depth-averaged velocity can be estimated using Shield's Curve. These are the shear stresses and velocities that will initiate sediment motion on a flat bed.

$$\tau_c = \rho\,[(sg-1)gD_{50}]\begin{cases} -0.005 + 0.0023\,d^* - 0.000378\,d^*\,ln(d^*) + \dfrac{0.23}{d^*} & \text{for } 0.22 \le d^* \le 150 \\ 0.0575 & \text{for } d^* > 150 \end{cases} \tag{B8}$$

$$d^* \equiv \left[(sg-1)g\,\frac{D_{50}^3}{\nu^2}\right]^{1/3}, \tag{B9}$$

where

$\tau_c \equiv$ critical bed shear stress (i.e. the shear stress that will initiate sediment motion),

$\rho \equiv$ mass density of the water (1.94 slugs/ft^3 fresh and 1.99 slugs/ft^3 salt STP) ,

$sg \equiv$ specific gravity of the sediment (Quartz sand in fresh water 2.655),

$g \equiv$ acceleration of gravity (32.174 ft/s^2),

$D_{50} \equiv$ Median diameter of sediment,

$\nu \equiv$ kinematic viscosity of water $\equiv \dfrac{\mu}{\rho}$ (1.076x10^{-5} ft^2/s fresh & 1.049x10^{-5} ft^2/s STP),

and

$\mu \equiv$ dynamic viscosity of water (2.09 x 10^{-5} lb$_f$ s/ft^2 STP).

For fully developed (water surface slope) driven flow under field conditions the relationship between depth-averaged velocity and bed shear stress is:

$$V = 2.5\sqrt{\frac{\tau}{\rho}}\,\ln_e\left(\frac{11.0\,y_0}{RR\,D_{50}}\right), \tag{B10}$$

where

RR $\equiv$ relative roughness of the bed (roughness height divided by the grain diameter).

Thus the critical depth-averaged velocity is,

$$V_c = 2.5\sqrt{\frac{\tau_c}{\rho}}\,\ln_e\left(\frac{11.0\,y_0}{RR\,D_{50}}\right). \tag{B11}$$

Note that y_0 and D_{50} must be in the same units.

Plots of critical velocity for range of parameters are presented in Figures B3 through B5.

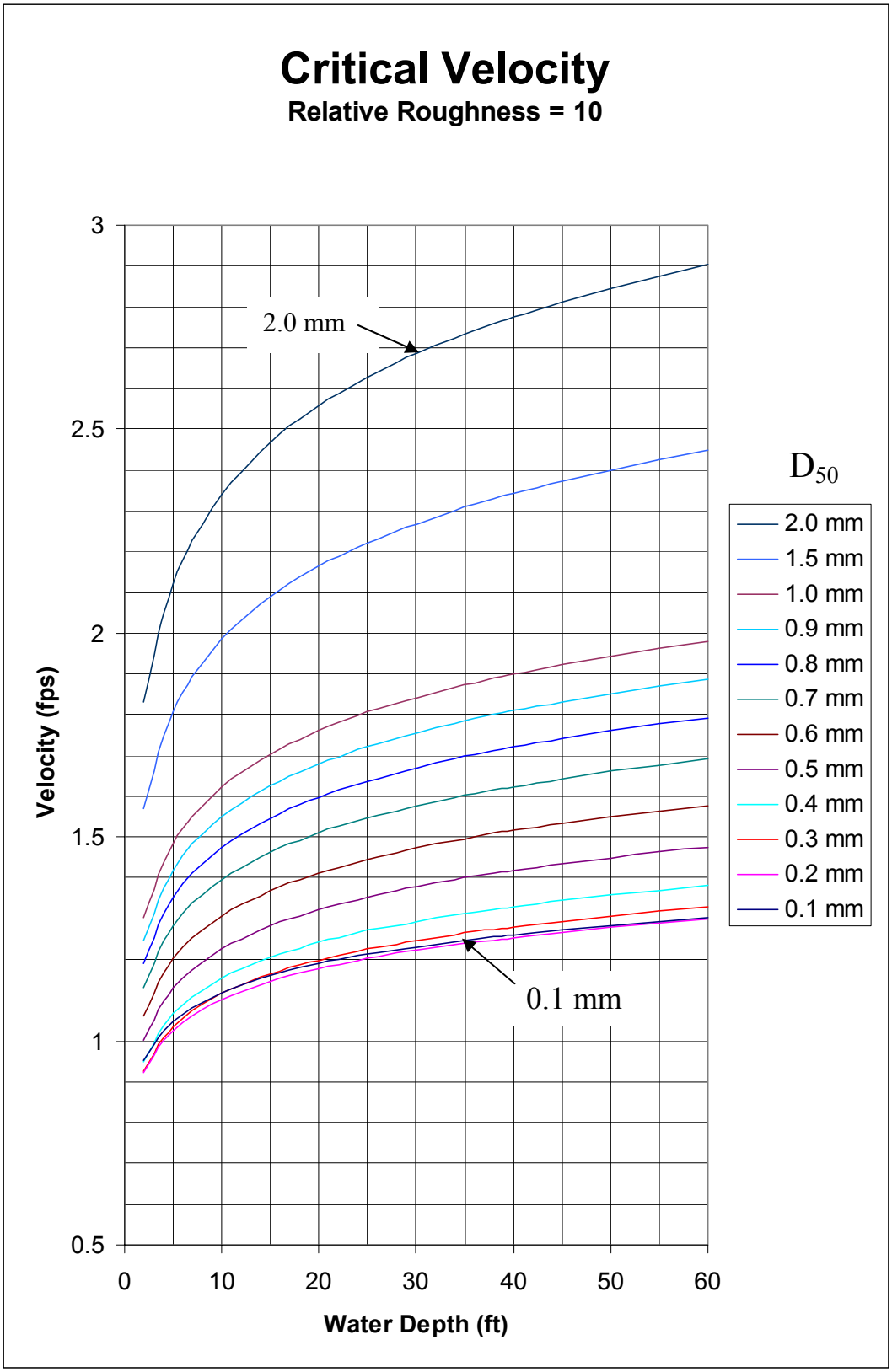

Figure B3. Critical velocity for relative roughness = 10 and various D_{50} sediment sizes for quartz sand and STP fresh water.

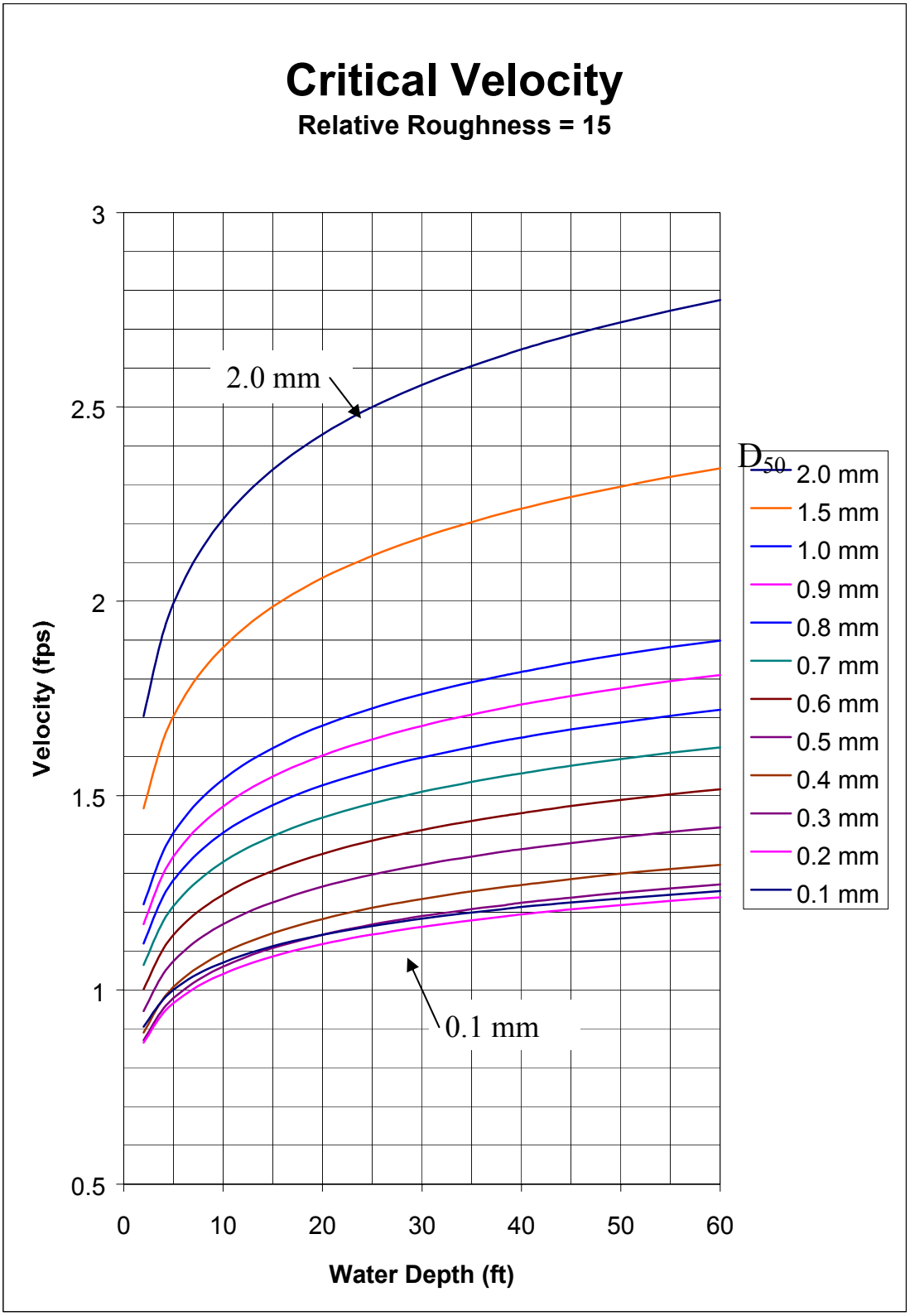

Figure B4. Critical velocity for Relative Roughness = 15 and various D_{50} sediment sizes for quartz sand and STP fresh water.

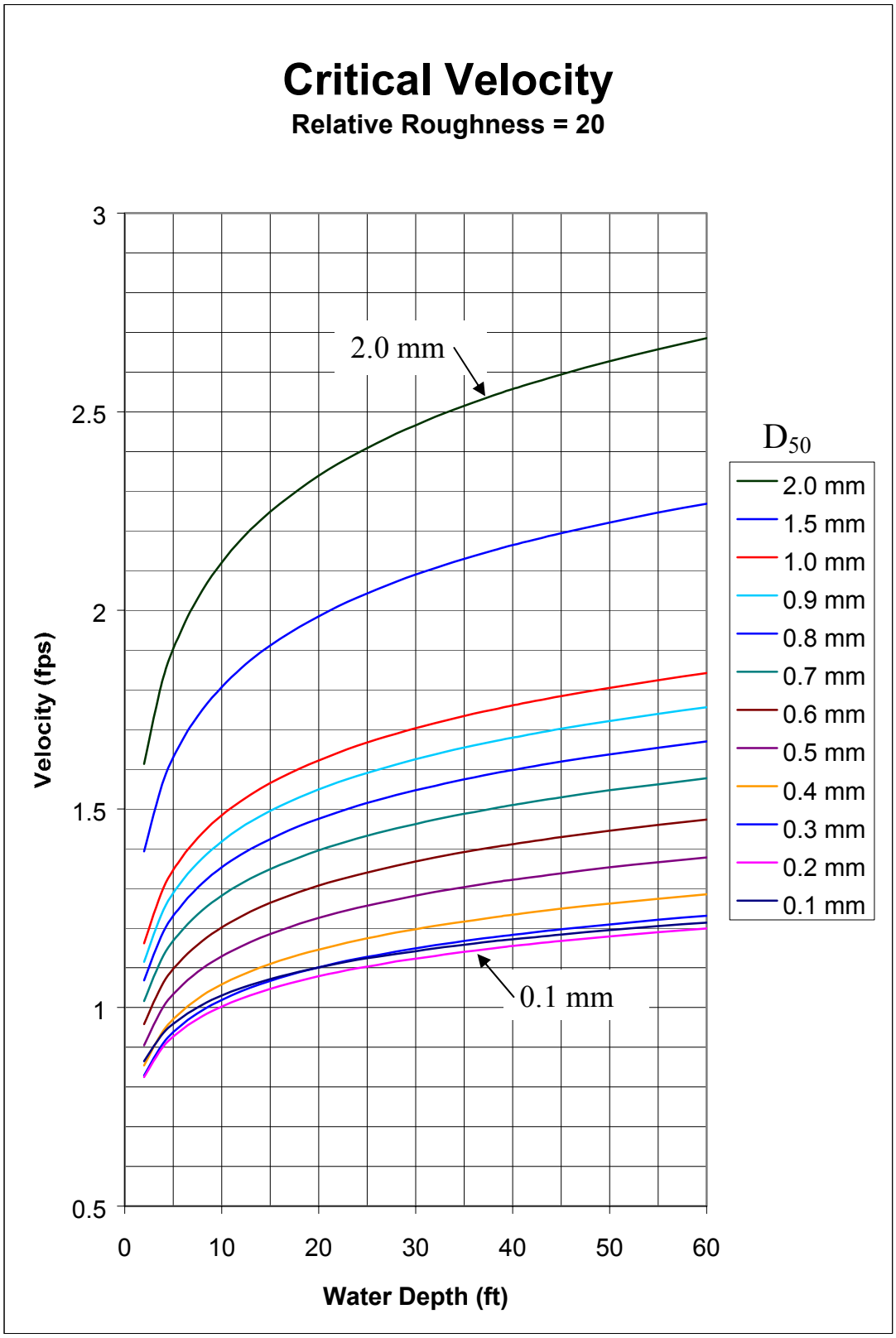

Figure B5. Critical velocity for relative roughness = 20 and various D_{50} sediment sizes for quartz sand and STP fresh water.

4.6 Live Bed Scour Peak Velocity

In van Rijn's (1993) method for estimating the depth-averaged velocity where the bed planes out two conditions must be satisfied, 1) the dimensionless parameter, T, must be greater than 25 and 2) the Froude Number must be greater than 0.8. The smallest velocity that will satisfy both criteria is the value to be used in the live bed local scour equations.

$$T \equiv \frac{\tau' - \tau_c}{\tau_c} \geq 25 \text{ and} \tag{B12}$$

$$Fr \geq 0.8, \tag{B13}$$

where

$$\tau' \equiv \rho g \left[\frac{V}{\left(18 \frac{m^{1/2}}{s} \right) \log_{10} \left(\frac{4y_0}{D_{90}} \right)} \right]^2 = \rho g \left[\frac{V}{\left(32.6 \frac{ft^{1/2}}{s} \right) \log_{10} \left(\frac{4y_0}{D_{90}} \right)} \right]^2, \tag{B14}$$

$\tau_c \equiv$ critical bed shear stress (obtained from Shield's Curve),

$$Fr \equiv \frac{V}{\sqrt{g y_0}} \text{ and} \tag{B15}$$

$D_{90} \equiv$ 90% of the sediment (by weight) has a diameter less than this value.

The smallest depth averaged velocity that will satisfy both conditions is the larger of the velocities computed as follows

$$\tau' \equiv \rho g \left[\frac{V}{\left(18 \frac{m^{1/2}}{s} \right) \log_{10} \left(\frac{4y_0}{D_{90}} \right)} \right]^2 = \rho g \left[\frac{V}{\left(32.6 \frac{ft^{1/2}}{s} \right) \log_{10} \left(\frac{4y_0}{D_{90}} \right)} \right]^2 = 25\tau_c + \tau_c = 26\tau_c \tag{B16}$$

Solving for V in this equation yields the first equation

Equation 1

$$V_1 = \sqrt{\frac{26\tau_c}{\rho g}}\left(18\frac{m^{1/2}}{s}\right)\log_{10}\left(\frac{4y_0}{D_{90}}\right) = \sqrt{\frac{26\tau_c}{\rho g}}\left(32.6\frac{ft^{1/2}}{s}\right)\log_{10}\left(\frac{4y_0}{D_{90}}\right), \quad \text{(B17)}$$

The second equation comes from the Froude Number criteria.

Equation 2

$$V_2 = 0.8\sqrt{gy_0} \quad \text{(B18)}$$

$$\boxed{V_{lp} = \text{the greater of } V_1 \text{ and } V_2.} \quad \text{(B19)}$$

Plots of V_{lp} versus water depth, y_0, for a range of quartz sediment diameters are given in Figures B6 and B7. These curves are based on Snamenskaya's (1969) results, which as stated above, are very close to the values obtained using van Rijn's method.

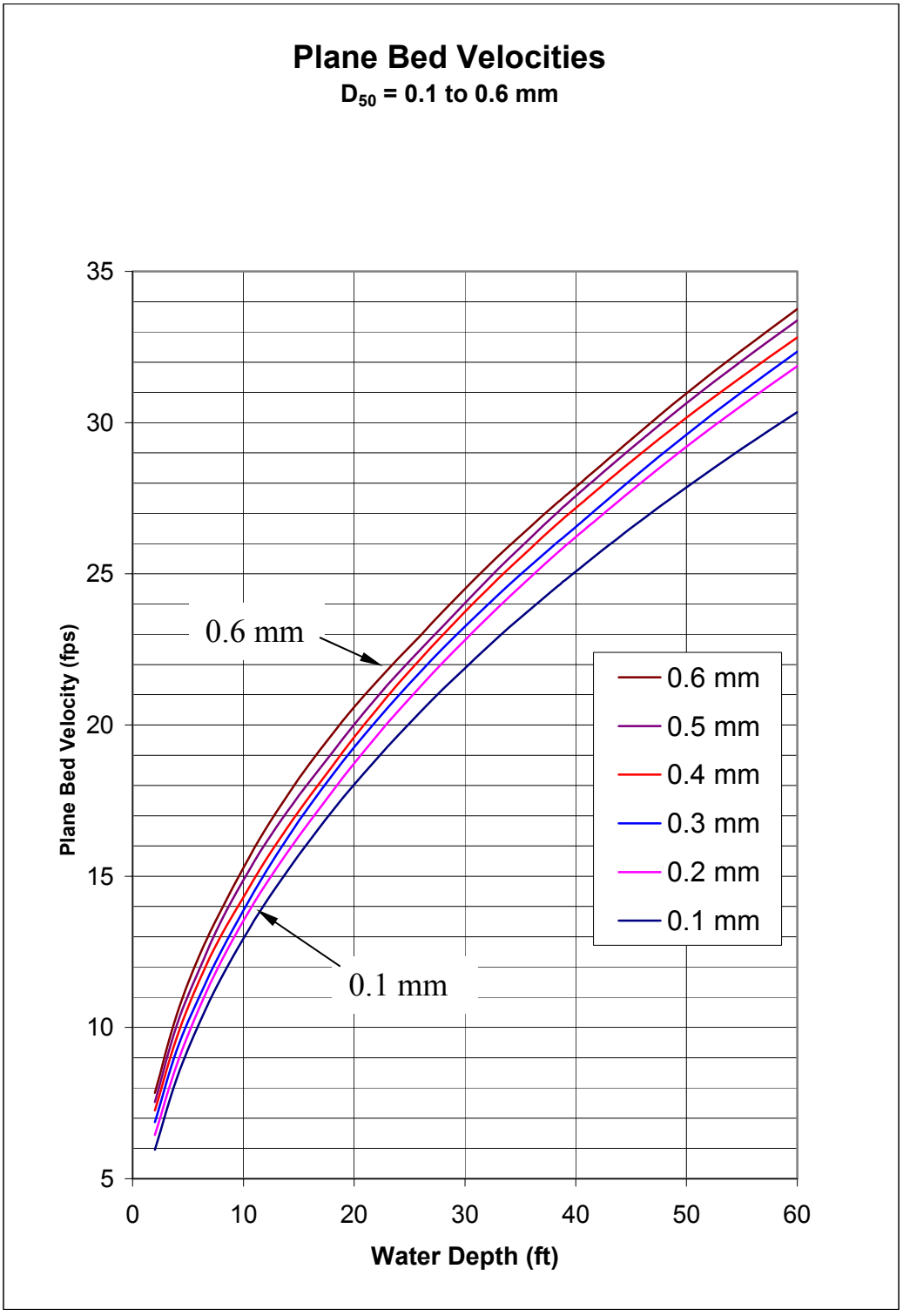

Figure B6. Plane bed velocity for D_{50} sediment sizes between 0.1 mm and 0.6 mm using Snamenskaya's (1969) results.

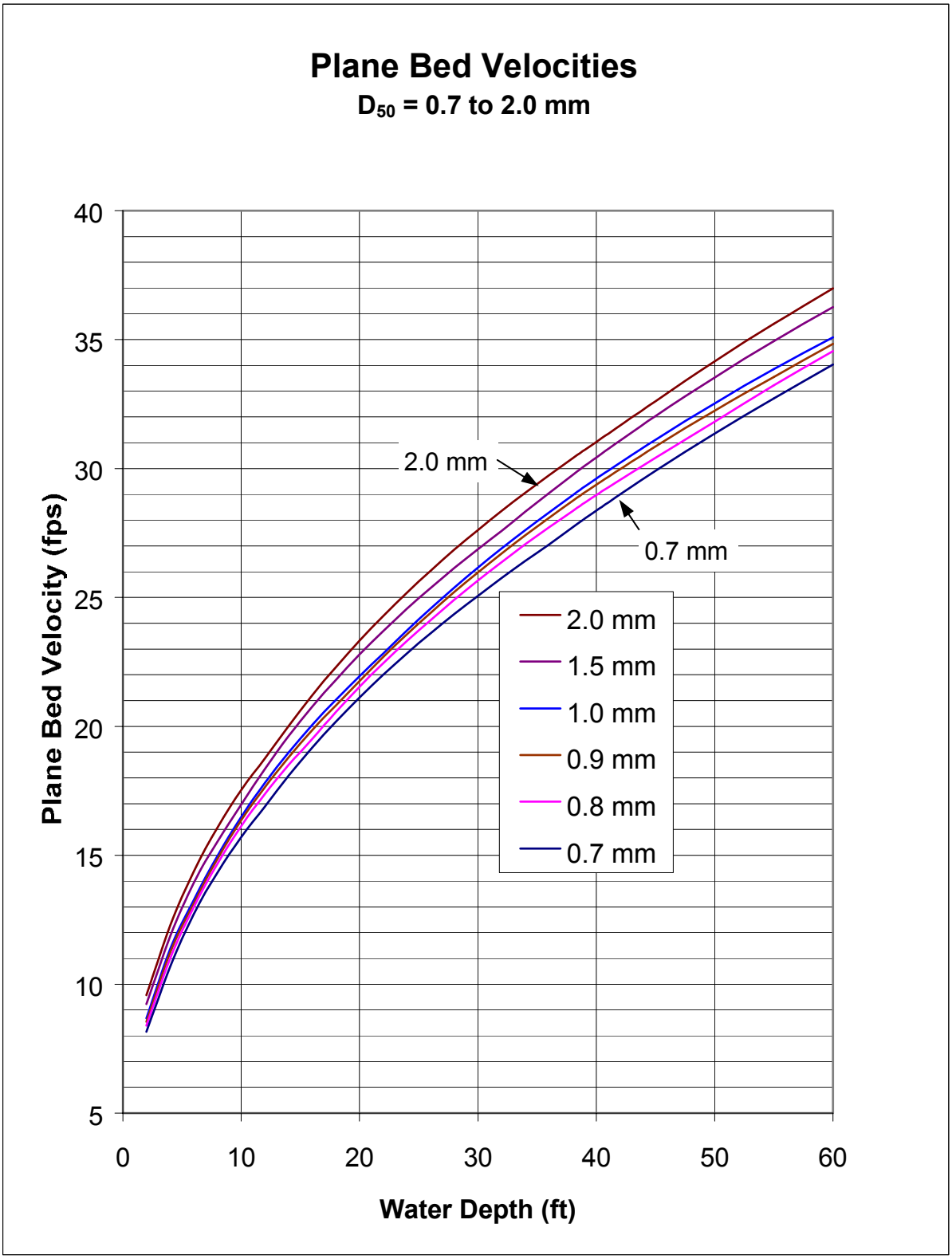

Figure B7. Plane bed velocity for D_{50} sediment sizes between 0.7 mm and 2.0 mm using Snamenskaya's (1969) results.